Astron. Astrophys. 53, 179—189 (1976)

ASTRONOMY
AND
ASTROPHYSICS

# Interstellar Formaldehyde in Southern Dark Dust Clouds

Aa. Sandqvist and K. P. Lindroos
Stockholm Observatory, S-13300 Saltsjöbaden, Sweden

Received October 1, revised November 25, 1975

**Summary.** A catalogue of 42 dark dust clouds of high visual opacity class has been compiled from a study of the Whiteoak Fields ($-33° > \delta > -46°$) of the National Geographic Society—Palomar Observatory Sky Survey, listing the equatorial and galactic coordinates of the cloud centers, the approximate areas and estimated opacity classes. Formaldehyde has been detected in 33 of the clouds by means of the molecule's 6-cm $1_{10} \rightarrow 1_{11}$ rotational transition and analysis of the hyperfine structure of the absorption profiles from 27 of the clouds has been performed. Half of the analysed clouds have a mean excitation temperature of 2.2 K while a third of the clouds have a lower mean excitation temperature of 1.9 K. From kinematical evidence it is concluded that most of the dark clouds, the Heeschen cold cloud of neutral hydrogen seen towards the Galactic center region and the local neutral hydrogen of low velocity dispersion are physically associated. The presence of a velocity gradient in a cloud complex lying in the constellation of Corona Australis is discussed.

**Key words:** dark clouds — formaldehyde — local system — interstellar molecules — Gould's Belt

## I. Introduction

The presence of formaldehyde ($H_2CO$) in interstellar dust clouds has been well established through the detection of absorption against the 2.7 K cosmic background radiation in the molecule's $1_{10} \rightarrow 1_{11}$ rotational transition at 4830 MHz. A comprehensive survey of formaldehyde in dust clouds listed in Lynds' (1962) Catalogue of Dark Nebulae has been published by Dieter (1973) who obtained values for velocities, optical depths, excitation temperatures and other parameters by analysing the observed profiles using the method of least squares applied to the six hyperfine components which make up the 6-cm $H_2CO$ transition. A similar analysis of a considerably smaller number of clouds has been performed by Heiles (1973). They obtain typical values for the excitation temperatures of about 2.5, 2.2 and 1.6 K, values considerably below the kinetic temperatures for the clouds and thus indicative of some nonequilibrium, process for the cooling excitation mechanism—possibly collisional.

The kinematical distribution of dark clouds surveyed in the 4830 MHz $H_2CO$ line has also been studied by Minn and Greenberg (1973) and Lindblad et al. (1973). The latter paper and Lindblad (1974) discuss the possible association of many of the dust clouds, the bright young stars comprising Gould's Belt and the local component of interstellar neutral hydrogen. In connection with a study of this system, Sandqvist and Lindblad (1976) have observed a large number of dark clouds along Gould's Belt in the 21-cm H I, 9-cm CH and 6-cm $H_2CO$ lines.

The dust clouds surveyed above are limited to the galactic longitude range of $353° - 0° - 240°$ by the mere limitation of sky coverage in declination ($\delta > -33°$) of the plates in the National Geographic Society—Palomar Observatory Sky Survey from which Lynds catalogued the clouds. The present paper extends this longitude range to $336° - 0° - 271°$ and the sky coverage to $\delta > -46°$ by presenting a catalogue of 42 southern dust clouds, in 33 of which formaldehyde has been detected. In 27 of these clouds the absorption is sufficiently strong to permit a detailed analysis of the hyperfine components of the 6-cm $H_2CO$ line and physical parameters for these clouds have been determined. The relation of these dust clouds to the local system of gas, dust and stars is discussed.

## II. Catalogue of Southern Dark Dust Clouds

In 1964, J. B. Whiteoak made a southern extension to the Palomar Sky Atlas by photographing 100 fields in the declination zones $-36°$ and $-42°$ with the 48-inch

*Send offprint requests to:* Aa. Sandqvist

**Table 1.** Southern dark dust clouds

| (1) Cloud | (2) $\alpha$ (1950.0) | (3) $\delta$ (1950.0) | (4) $l$ | (5) $b$ | (6) Area (sq. deg.) | (7) Opacity class | (8) Barnard number |
|---|---|---|---|---|---|---|---|
| 1 | $8^h37^m.2$ | −40°33′ | 260°.41 | 0°.44 | 0.013 | 5 | |
| 2 | 8 42.8 | −41 07 | 261.51 | 0.92 | 0.004 | 5 | |
| 3 | 8 52.2 | −41 34 | 262.98 | 1.99 | 0.008 | 4 | |
| 4 | 8 51.8 | −42 02 | 263.29 | 1.64 | 0.071 | 5 | |
| 5 | 9 36.2 | −45 33 | 271.40 | 4.93 | >0.130 | 4 | |
| 6 | 15 54.8 | −42 27 | 335.69 | 8.09 | 0.027 | 5 | |
| 7 | 15 58.4 | −41 44 | 336.68 | 8.19 | 0.048 | 6 | |
| 8 | 16 10.7 | −43 56 | 336.87 | 5.05 | 0.030 | 6 | |
| 9 | 16 04.5 | −41 34 | 337.65 | 7.56 | 0.056 | 5 | |
| 10 | 16 08.0 | −41 35 | 338.12 | 7.10 | 0.028 | 6 | |
| 11 | 15 53.7 | −37 39 | 338.71 | 11.87 | 0.013 | 6 | |
| 12 | 15 39.5 | −34 00 | 338.84 | 16.51 | 0.067 | 6 | B 228 |
| 13 | 15 42.5 | −34 19 | 339.14 | 15.88 | 0.071 | 5 | B 228 |
| 14 | 16 06.2 | −38 59 | 339.66 | 9.24 | 0.052 | 6 | |
| 15 | 16 43.0 | −44 25 | 340.52 | 0.53 | 0.006 | 6 | B 235 |
| 16 | 16 21.6 | −39 54 | 341.16 | 6.50 | 0.019 | 6 | |
| 17 | 16 49.4 | −43 30 | 341.96 | 0.24 | 0.013 | 5 | |
| 18 | 16 41.3 | −40 17 | 343.44 | 3.47 | 0.006 | 5 | B 44a |
| 19 | 16 55.7 | −42 22 | 343.57 | 0.06 | 0.026 | 5 | |
| 20 | 16 57.5 | −40 43 | 345.07 | 0.83 | 0.036 | 5 | B 48 |
| 21 | 16 33.6 | −35 30 | 346.03 | 7.78 | 0.006 | 6 | B 231 |
| 22 | 17 22.7 | −42 35 | 346.35 | − 4.07 | 0.027 | 5 | B 263 |
| 23 | 17 07.7 | −40 33 | 346.38 | − 0.61 | 0.039 | 6 | B 58 |
| 24 | 16 34.2 | −35 06 | 346.41 | 7.96 | 0.004 | 6 | B 231 |
| 25 | 16 40.8 | −35 15 | 347.20 | 6.84 | 0.039 | 5 | B 233 |
| 26 | 17 30.7 | −40 23 | 349.02 | − 4.10 | 0.019 | 5 | |
| 27 | 16 59.7 | −36 02 | 349.03 | 3.37 | 0.027 | 4 | |
| 28 | 17 31.8 | −39 12 | 350.13 | − 3.64 | 0.022 | 5 | |
| 29 | 17 31.8 | −39 11 | 350.14 | − 3.63 | 0.024 | 4 | |
| 30 | 16 59.7 | −34 22 | 350.35 | 4.39 | 0.017 | 6 | B 50 |
| 31 | 16 59.5 | −33 12 | 351.25 | 5.14 | 0.008 | 5 | B 49 |
| 32 | 17 02.8 | −33 11 | 351.68 | 4.60 | 0.016 | 4 | B 53 |
| 33 | 17 18.6 | −35 33 | 351.69 | 0.57 | 0.013 | 5 | B 257 |
| 34 | 17 14.9 | −34 55 | 351.77 | 1.56 | 0.012 | 5 | |
| 35 | 17 14.2 | −34 39 | 351.91 | 1.83 | 0.103 | 4 | |
| 36 | 17 40.5 | −33 24 | 355.97 | − 2.01 | 0.008 | 5 | |
| 37 | 17 43.6 | −33 48 | 355.97 | − 2.77 | 0.090 | 4 | |
| 38 | 17 43.7 | −32 55 | 356.73 | − 2.33 | 0.058 | 5 | |
| 39 | 19 00.8 | −37 23 | 359.75 | −18.40 | 0.057 | 5 | |
| 40 | 18 59.5 | −37 11 | 359.85 | −18.09 | 0.062 | 5 | |
| 41 | 18 57.8 | −36 59 | 359.92 | −17.70 | 0.031 | 6 | |
| 42 | 19 06.9 | −37 13 | 360.37 | −19.48 | 0.033 | 6 | |

Schmidt telescope. Only red plates with a maximum response near 6500 Å were obtained and since the minimum zenith distance was 66° the plates are of lower quality than those of the Palomar Sky Atlas itself. But they are of sufficiently good quality to determine the positions of dark nebulae and to obtain their approximate areas and opacity classes. Since the ultimate purpose of our project was to survey the clouds for formaldehyde, only the darker clouds (and therefore those more likely to contain detectable formaldehyde) were chosen. Estimates for the opacity class on a scale from 1 to 6 were made, but since no blue plates were available these estimates must be considered more uncertain than those made by Lynds for her catalogue, although a serious attempt was made to follow her scale as closely as possible.

Table 1 contains the 42 dark dust clouds chosen from the "Whiteoak Fields". In Column (1) is the number of the cloud. The 1950.0 equatorial coordinates of the center of the cloud is given in Columns (2) and (3) with the corresponding galactic coordinates given in Columns (4) and (5). The approximate area in square degrees is given in Column (6) and the opacity class, on a scale from 1 to 6 with 6 as the apparently darkest, is listed in Column (7). The Barnard (1927) number of an object coincident with a specific cloud is given in Column (8).

## III. Formaldehyde Observations

The observations were made in November 1972 with the 42.7-m radio telescope of the National Radio

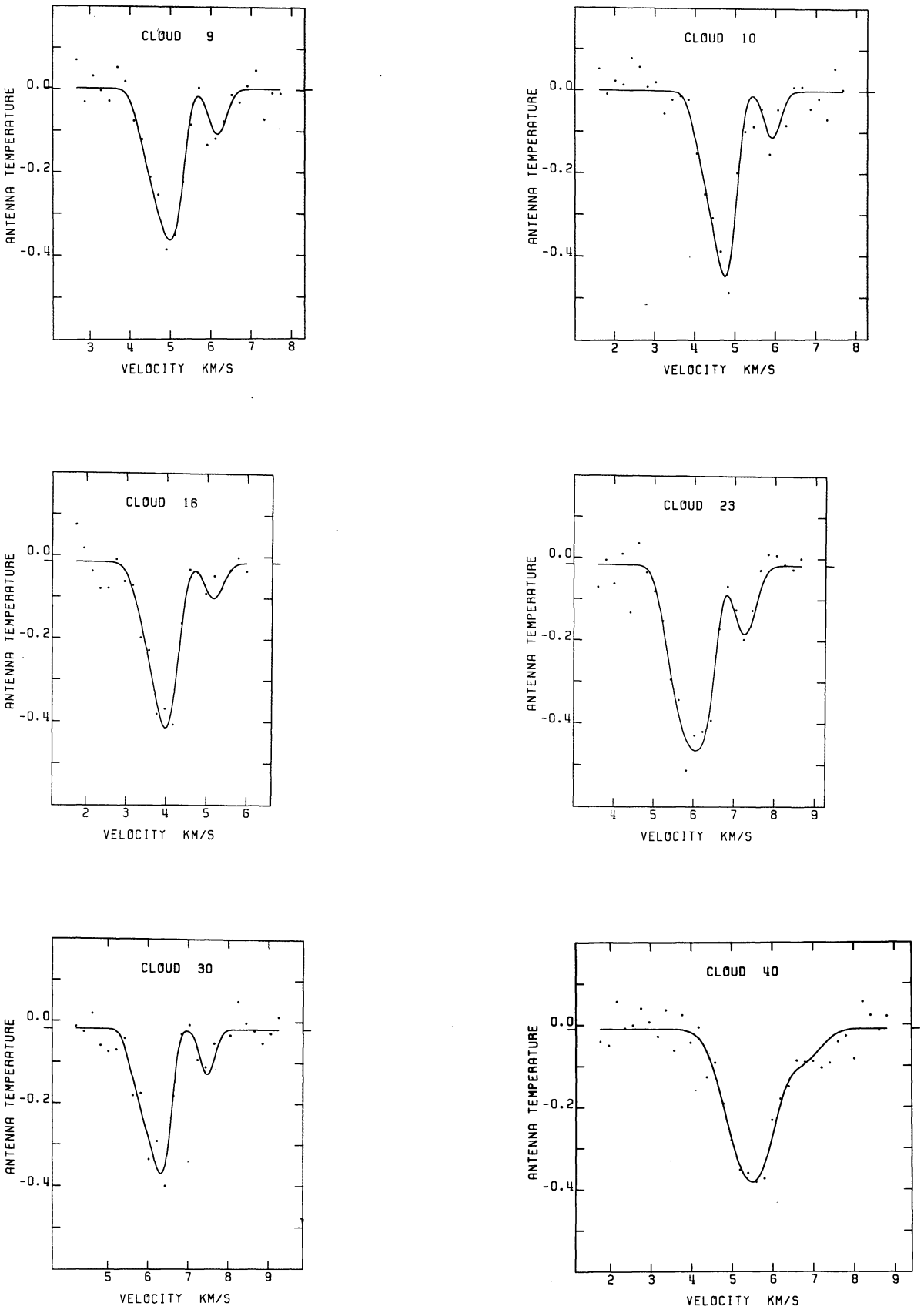


**Fig. 1.** The observed profile (dots) of the 6-cm $H_2CO$ line with the best fit (solid line) to the data of a theoretical line with six hyperfine components, for six southern clouds

Astronomy Observatory[1] (NRAO), Green Bank, West Virginia. The beamwidth is 6'.6 at 4830 MHz and the beam efficiency, $\eta_B$, is approximately 80%. The NRAO TRG cooled parametric amplifier was used in conjunction with the 413-channel autocorrelation receiver, and the total system temperature was generally close to 65 K. The autocorrelator served in the "parallel" mode with two receiver bands ($A$ and $B$) each containing 192 channels. Receivers $A$ and $B$ spanned velocity ranges of $(-40, +30)$ and $(-20, +15)$ km s$^{-1}$, respectively with channel resolutions of 7.9 and 3.94 kHz or 0.49 and 0.24 km s$^{-1}$, respectively. The frequency switching observing method was used with the signal and reference bands overlapping to such an extent that the expected line profile was being observed in both halves of the switching cycle, thus effectively doubling the integration time to 90 min which results in a profile RMS noise value of about 0.03 K.

## IV. Analysis of Hyperfine Structure

The profiles of 27 clouds were analysed by means of the 6 hyperfine components of the $1_{10}\rightarrow 1_{11}$ $H_2CO$ transition in a manner similar to that of Dieter (1973) and Heiles (1973). The most intense component, $F:2\rightarrow 2$, is used as a standard and has a rest frequency of 4829.65961 MHz (Tucker et al., 1971). Conversion of the frequency scale to a scale of velocity with respect to the local standard of rest was performed assuming the "standard" solar motion of 20 km s$^{-1}$ towards the apex $\alpha(1900.0)=18^h00^m$ and $\delta(1900.0)=+30°$. A given profile can be considered to consist of six gaussian components corresponding to the six hyperfine components of the line, and the resultant antenna temperature, $\Delta T$, in Kelvins as a function of velocity, $v$, in km s$^{-1}$ can be represented by

$$\Delta T(v)=\left(\eta_B\frac{\Omega_c}{\Omega_B}\right)(T_x-T_c)\cdot\left[\left[1-\exp\left\{-\tau_m\sum_{i=1}^{6}\alpha_i\exp\left[-\frac{1}{2}\left(\frac{v-v_i-V}{\sigma}\right)^2\right]\right\}\right]+K, \quad (1)$$

where $\eta_B=0.8$ is the beam efficiency, $\Omega_c/\Omega_B$ is the fraction of the main beam occupied by the cloud, $T_x$ is the excitation temperature, $T_c$ is the background continuum temperature assumed to be 2.7 K, $\tau_m$ is the optical depth of the main component ($F:2\rightarrow 2$), $\alpha_i$ is the ratio of the optical depth of component $i$ to that of the main component, and $v_i$ is the velocity separation of each component from the main one (both $\alpha_i$ and $v_i$ are derived from values given by Tucker et al., 1971), $V$ is the radial velocity of the cloud, and $\sigma$ is the velocity dispersion which is assumed to be the same for all the components, $K$ is a constant which accounts for small zero-level errors.

Values for the parameters $T_x$, $\tau_m$, $V$ and $\sigma$ were obtained by fitting Equation (1) to the profiles by the method of least squares assuming local thermodynamic equilibrium (LTE) in the clouds. A second somewhat simpler, but more time-consuming, minimizing program was used in some cases where the least squares method resulted in negative values for $T_x$ and $\tau_m$. Figure 1 shows some typical spectra (dots) and the fitted profiles computed from Equation (1) (solid lines).

Following Scoville et al. (1972) we now define the equivalent width of the line as

$$W=\int_{\text{line}}\{1-\exp[-\tau_t(v)]\}\,dv. \quad (2)$$

Here, $\tau_t$ is the optical depth for the total 6-cm transition, rather than for the main hyperfine component alone, and it is given by

$$\tau_t(v)=\tau_m\sum_{i=1}^{6}\alpha_i\exp\left[-\frac{1}{2}\left(\frac{v-v_i-V}{\sigma}\right)^2\right]. \quad (3)$$

The column density $N_1$ of $H_2CO$ molecules in the lower of the 6-cm transition divided by the excitation temperature can be derived from Equation (3) of Scoville et al. and is given by

$$\frac{N_1}{T_x}=1.25\,10^{13}\quad W\cdot\frac{\tau_t(V)}{1-\exp\{-\tau_t(V)\}}, \quad (4)$$

where the factor $\tau_t(V)/[1-\exp\{-\tau_t(V)\}]$ is a correction for finite optical depth. A minimum value for the total column density $N_{H_2CO}$ of ortho and para molecules is given by $N_{H_2CO}=3.1\,N_1$ assuming a normal ortho-para ratio and energy level populations according to a Boltzman temperature of 2.7 K (Scoville et al., 1972).

In Table 2, we present a summary of the formaldehyde observations and the values of parameters derived from the hyperfine analysis. The content of the table is as follows: Column (1), the cloud's number; Column (2), the fraction of the main beam that the cloud occupies; Column (3), the antenna temperature of the maximum absorption; Column (4), full linewidth at half intensity; Column (5), the equivalent width of the line; Column (6), the cloud's radial velocity with respect to the local standard of rest; Column (7), the velocity dispersion of each hyperfine component; Column (8), the optical depth of the main ($F:2\rightarrow 2$) hyperfine component; Column (9), the optical depth for the total 6-cm transition at the radial velocity of the cloud; Column (10), the excitation temperature of the $1_{10}\rightarrow 1_{11}$ $H_2CO$ transition; Column (11), the column density of $H_2CO$ molecules in the lower level of the 6-cm transition divided by the excitation temperature; Column (12), a minimum value for the total column density of ortho- and paraformaldehyde molecules; Column (13), remarks defined at the bottom of the table.

[1] Operated by Associated Universities, Inc., under contract with the National Science Foundation

**Table 2.** Formaldehyde observations and derived parameters

| (1) Cloud | (2) $\Omega_c/\Omega_B$ | (3) $\Delta T_{max}$ (K) | (4) $\Delta V$ (km s$^{-1}$) | (5) $W$ (km s$^{-1}$) | (6) $V$ (km s$^{-1}$) | (7) $\sigma$ (km s$^{-1}$) | (8) $\tau_m$ | (9) $\tau_t(V)$ | (10) $T_x$ (K) | (11) $N_1/T_x$ ($\times 10^{13}$ cm$^{-2}$ K$^{-1}$) | (12) $N_{H_2CO}$ ($\times 10^{13}$ cm$^{-2}$) | (13) Remarks |
|---|---|---|---|---|---|---|---|---|---|---|---|---|
| 1 | 0.97 | −0.10? | 0.8 | | 6.8 | | | | | | | C |
| 2 | 0.37 | — | — | | | | | | | | | Q |
| 3 | 0.61 | — | — | | | | | | | | | Q |
| 4 | 1 | −0.38 | 2.8 | 1.339 | 5.24 | 1.08 | 0.25 | 0.55 | 1.64 | 2.18 | 11.04 | A, N |
| 5 | 1 | −0.20 | 1.6 | 1.166 | −2.91 | 0.40 | 0.71 | 1.24 | 2.27 | 2.55 | 17.93 | |
| 6 | 1 | −0.21 | 0.9 | 0.285 | 4.93 | 0.26 | 0.20 | 0.31 | 1.77 | 0.41 | 2.27 | A, N |
| 7 | 1 | −0.37 | 1.2 | 0.744 | 4.37 | 0.24 | 0.72 | 1.07 | 2.04 | 1.52 | 9.59 | |
| 8 | 1 | −0.22 | 1.2 | 0.778 | 4.23 | 0.29 | 0.60 | 0.95 | 2.20 | 1.51 | 10.28 | |
| 9 | 1 | −0.38 | 0.9 | 0.869 | 5.04 | 0.21 | 1.02 | 1.47 | 2.11 | 2.07 | 13.55 | |
| 10 | 1 | −0.47 | 0.9 | 0.580 | 4.79 | 0.20 | 0.61 | 0.87 | 1.74 | 1.09 | 5.87 | |
| 11 | 0.92 | −0.34 | 1.0 | 0.208 | 4.73 | 0.25 | 0.15 | 0.23 | 0.56 | 0.29 | 0.50 | N |
| 12 | 1 | −0.46 | 1.6 | 0.520 | 5.34 | 0.47 | 0.21 | 0.39 | 0.92 | 0.78 | 2.23 | |
| 13 | 1 | −0.35 | 1.1 | 0.623 | 4.48 | 0.29 | 0.45 | 0.71 | 1.88 | 1.09 | 6.35 | A |
| 14 | 1 | −0.29 | 1.3 | 1.025 | 4.64 | 0.28 | 0.92 | 1.45 | 2.26 | 2.42 | 17.01 | |
| 15 | 0.46 | −0.18, −0.14 | 0.7, 0.6 | | 4.9, 6.3 | | | | | | | C, D |
| 16 | 1 | −0.38 | 1.0 | 0.433 | 4.04 | 0.23 | 0.37 | 0.55 | 1.53 | 0.70 | 3.33 | |
| 17 | 0.92 | Not observed | | | | | | | | | | |
| 18 | 0.46 | −0.20 | 0.8 | 0.364 | 4.72 | 0.28 | 0.25 | 0.39 | 1.21 | 0.55 | 2.06 | N |
| 19 | 1 | −0.30 | 0.7 | 0.731 | 5.93 | 0.21 | 0.84 | 1.19 | 2.17 | 1.56 | 10.51 | A |
| 20 | 1 | −0.32 | 0.9 | 0.393 | 6.18 | 0.20 | 0.39 | 0.55 | 1.75 | 0.64 | 3.47 | |
| 21 | 0.41 | — | — | | | | | | | | | Q |
| 22 | 1 | −0.28 | 1.0 | 1.282 | 7.71 | 0.21 | 1.98 | 2.87 | 2.34 | 4.87 | 35.33 | |
| 23 | 1 | −0.47 | 1.2 | 1.318 | 6.12 | 0.26 | 1.61 | 2.46 | 2.09 | 4.44 | 28.74 | |
| 24 | 0.31 | — | — | | | | | | | | | Q |
| 25 | 1 | −0.19 | 1.8 | 1.439 | 4.83 | 0.42 | 0.94 | 1.67 | 2.42 | 3.70 | 27.73 | |
| 26 | 1 | −0.07 | 3.4 | | −5.1 | | | | | | | C |
| 27 | 1 | Not observed | | | | | | | | | | |
| 28 | 1 | −0.27 | 1.3 | 1.537 | −5.76 | 0.26 | 2.22 | 3.40 | 2.37 | 6.75 | 49.66 | A |
| 29 | 1 | −0.20 | 1.8 | 0.710 | −5.58 | 0.37 | 0.40 | 0.68 | 2.04 | 1.23 | 7.76 | A, N |
| 30 | 1 | −0.36 | 1.1 | 0.764 | 6.34 | 0.18 | 1.05 | 1.44 | 2.13 | 1.80 | 11.86 | |
| 31 | 0.56 | — | — | | | | | | | | | Q |
| 32 | 1 | Not observed | | | | | | | | | | |
| 33 | 0.92 | −0.11 | 1.5 | | 5.8 | | | | | | | C |
| 34 | 0.87 | −0.39 | 1.3 | 0.820 | 7.95 | 0.40 | 0.44 | 0.77 | 1.79 | 1.47 | 8.17 | A, N |
| 35 | 1 | −0.20 | 1.6 | 0.583 | 9.54 | 0.46 | 0.25 | 0.45 | 2.05 | 0.91 | 5.76 | A, N |
| 36 | 0.56 | −0.12 | 1.0 | | 3.8 | | | | | | | C |
| 37 | 1 | −0.13 | 1.6 | | −8.1 | | | | | | | C |
| 38 | 1 | — | — | | | | | | | | | Q |
| 39 | 1 | −0.34 | 1.2 | 1.045 | 5.57 | 0.31 | 0.84 | 1.36 | 2.12 | 2.39 | 15.69 | |
| 40 | 1 | −0.36 | 1.4 | 1.019 | 5.61 | 0.42 | 0.55 | 0.98 | 1.97 | 2.00 | 12.17 | |
| 41 | 1 | −0.18 | 1.9 | 0.540 | 6.12 | 0.39 | 0.27 | 0.47 | 2.02 | 0.85 | 5.29 | |
| 42 | 1 | −0.29 | 0.9 | 1.127 | 5.54 | 0.18 | 1.89 | 2.61 | 2.34 | 3.97 | 28.81 | A |

A – the profile in receiver bank *A* was used in the hyperfine analysis
N – the least squares method was not used in the hyperfine analysis
C – no hyperfine analysis was performed. Error in $V$ is less than $\pm 0.2$ km s$^{-1}$
D – two velocity components
Q – observed, but not detected

Hyperfine analysis was done on profiles with $-0.18\ \text{K} \geqq \Delta T_{max} \geqq -0.47\ \text{K}$ and the signal-to-RMS noise in these profiles ranges from 4:1 to 12:1. Errors for the derived parameters were determined by plotting the residuals between the reduced and the theoretical profiles for different values of the parameters, varying the parameters one at a time. Upper and lower limits to the parameters were then determined by eye inspection of the residuals in a manner similar to Heiles (1973) and we find typical errors in $T_x$, $\tau_m$, and $\sigma$ to be 25% and in $V$ to be 0.1 km s$^{-1}$. The real errors in $T_x$ and $\tau_m$ and in the other parameters derived from these two, e.g. $N_{H_2CO}$, may be considerably larger due to the uncertainties in the assumptions concerning the physical structures of the clouds and the populations of the formaldehyde energy levels.

## V. Discussion

### *a) Parameters of Southern Dark Dust Clouds*

Three fourths of the clouds in Table 1 lie at positive galactic latitudes continuing the tendency, discussed by

**Table 3.** Distribution of cloud parameters

| $W$ (km s$^{-1}$) | % | cf. % (Scoville et al., 1972) |
|---|---|---|
| 0–0.5 | 26 | 20 |
| 0.6–1.0 | 48 | 13 |
| 1.1–1.5 | 26 | 0 |
| >1.5 | 0 | 67 |

| $\sigma$ (km s$^{-1}$) or [kHz] | % | cf. % (Dieter, 1973) |
|---|---|---|
| 0.04–0.15 [1–2] | 0 | 6 |
| 0.16–0.27 [3–4] | 44 | 26 |
| 0.28–0.39 [5–6] | 30 | 31 |
| 0.40–0.51 [7–8] | 22 | 15 |
| >0.52 [ >8] | 4 | 22 |

| $\tau_m$ | % | cf. % (Dieter, 1973) |
|---|---|---|
| <0.1 | 0 | 16 |
| 0.1–0.5 | 44 | 45 |
| 0.6–1.0 | 37 | 21 |
| 1.1–1.5 | 4 | 9 |
| 1.6–2.0 | 11 | 3 |
| >2.0 | 4 | 5 |

| $N_1/T_x$ ($\times 10^{13}$ cm$^{-2}$ K$^{-1}$) | % | cf. % (Dieter, 1973) |
|---|---|---|
| 0.1–2.0 | 63 | 58 |
| 2.1–4.0 | 26 | 16 |
| 4.1–6.0 | 7 | 7 |
| 6.1–8.0 | 4 | 2 |
| >8.0 | 0 | 17 |

| $T_x$ (K) | % | cf. % (Dieter, 1973) | cf. % (Heiles, 1973) |
|---|---|---|---|
| ≦1.5 | 15 | 0 | 20 |
| 1.6–2.0 | 37 | 10 | 50 |
| 2.1–2.5 | 48 | 80 | 30 |
| >2.5 | 0 | 10 | 0 |

Lynds (1962), for the smallest clouds to lie slightly above the galactic plane. The mean galactic latitude, weighted by the area and opacity class, of the 42 clouds is $\bar{b}_w = +1.^\circ 4$. If one divides the clouds into three groups according to positions one obtains (i) 5 clouds in the galactic longitude range $260^\circ < l < 272^\circ$ have $\bar{b}_w = 3.^\circ 3$, (ii) 33 clouds in $335^\circ < l < 357^\circ$ have $\bar{b}_w = 4.^\circ 8$ and (iii) the Corona Australis (Cr A) clouds at $l = 0^\circ$ have $\bar{b}_w = -18.^\circ 4$.

Lynds (1962) found that the average area of the clouds of a specific opacity class decreased as the value of that class increased. This relation is also present in the clouds listed in Table 1. However, the 14 clouds with opacity class 6 and the 21 clouds with opacity class 5 have average areas of 0.028 and 0.031 square degrees, respectively while Lynds' clouds of opacity classes 6 and 5 average areas of 0.029 and 0.054 square degrees, respectively, the latter value being much closer to our value of 0.056 for the 7 clouds of our opacity class 4. This should be compared with Lynds' value of 0.358 for her opacity class 4. Judging solely from these average areas it would seem likely that our opacity class 4 and Lynds' opacity class 5 are comparable while our classes of 5 and 6 are comparable with Lynds' opacity class 6. This difference will have no significance for the following discussion of the statistical behaviour of the parameters of the clouds, since all the clouds will be considered together regardless of their opacity class.

In Table 3, we present the statistical distributions for the cloud parameters—$W$, $\sigma$, $\tau_m$, $N_1/T_x$, $T_x$—and make comparisons with parameter distributions for the clouds observed by Scoville et al. (1972), Dieter (1973) and Heiles (1973).

The equivalent width, $W$, shows a smooth distribution with a maximum in the range of 0.6–1.0 km s$^{-1}$. Scoville et al. (1972), who observed formaldehyde clouds in absorption against continuum sources in the longitude range $359^\circ < l < 2^\circ$, obtained equivalent widths which show two distinct frequency distributions. One third of their clouds fall in the range of our clouds, but the other two thirds have equivalent widths of between 2 and 31 km s$^{-1}$ and seem to form a distinct group of their own. Most of the clouds in the latter group have very high absolute radial velocities (20–150 km s$^{-1}$) and are most likely associated with the central region of the Galaxy. Their extraordinary large equivalent widths are due partly to the higher molecular densities present in the central regions of the Galaxy which in some cases cause saturation of the spectral lines, and partly to the velocity effects experienced by clouds near the Galactic center which result in wide spectral lines (see e.g. Sandqvist, 1974).

The velocity dispersion, $\sigma$, shows an unambiguous maximum with about half the clouds having values in the range of 0.16–0.27 km s$^{-1}$ (3–4 kHz) in contrast to Dieter who obtained values more evenly distributed over the ranges shown in Table 3. (Our instrumental $\sigma$ had a value of 0.1 km s$^{-1}$ in most cases.) It is likely that this difference in the distributions reflects our selection of clouds of higher opacity class. The full linewidth at half intensity is influenced by the known velocity separation of the hyperfine components, the optical depth and the velocity dispersion.

The frequency distribution for the optical depth, $\tau_m$, of the main hyperfine component shows that four fifths of our clouds are fairly evenly distributed in the range 0.1–1.0 while only two thirds of Dieter's fall in this range with a strong concentration to the range of 0.1–0.5. Our choice of high opacity class clouds seems to have augmented the number of clouds in the range 0.6–1.0 at the cost of losing all clouds with $\tau_m < 0.1$. This may imply a possible correlation of $\tau_m$ with visual opacity.

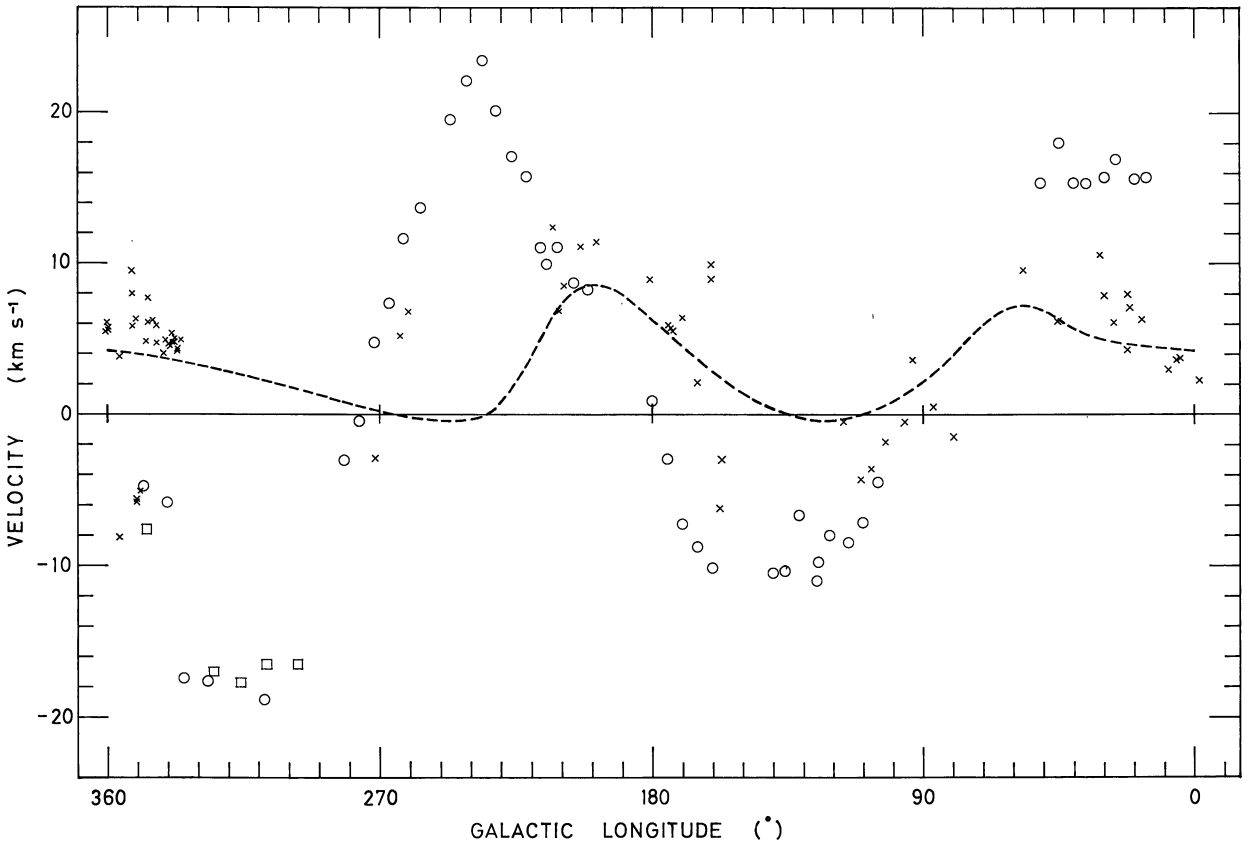


**Fig. 2.** Velocity—longitude diagram for the local interstellar matter. Lindblad et al.'s (1973) theoretical relation for Feature *A* of the local H I (dashed line), tentative velocities for the "other local feature" chosen from H I observations of various authors (open circles and squares), and observed velocities of dark clouds (crosses)

Almost two thirds of our clouds have ratios of column density to excitation temperature, $N_1/T_x$, which fall in the range of $0.1\ 10^{13}$–$2.0\ 10^{13}\ cm^{-2}\ K^{-1}$. Our only major disagreement with Dieter in this parameter is in the range of $N_1/T_x > 8.0\ 10^{13}\ cm^{-2}\ K^{-1}$ where we have no clouds but where Dieter has 17% of hers. Values this high are not representative of clouds in our part of the Galaxy but reflect the conditions nearer the Galactic center (Scoville et al., 1972; Fomalont and Weliachew, 1973) where $N_1/T_x$ can be as high as $98\ 10^{13}\ cm^{-2}\ K^{-1}$.

Half of our clouds have excitation temperatures, $T_x$, in the range of 2.1–2.5 K with an average value of 2.2 K and one third have $T_x$ in the range of 1.6–2.0 K with an average value of 1.9 K. This result appears to be a compromise between Dieter who favours higher excitation temperatures (although she classes them as upper limits) and Heiles who favours lower values. There is a definite lack of clouds with both low excitation temperature and high optical depth. This may reflect a prediction by the collisional pumping mechanism for the abnormal cooling of the 6-cm $H_2CO$ transition in dark clouds, viz. that the excitation temperature should increase with increasing density (Evans et al., 1975).

*b) Kinematics*

Lindblad et al. (1973) suggested that some of the dark clouds, the local neutral hydrogen (Feature *A*) and Gould's Belt of early type stars may be related and that this local, now, expanding, system may have had as its origin the passage of interstellar gas through the galactic shock located at the position of the Carina spiral arm, $60\ 10^6$ years ago. To illustrate the relation between some of the dark clouds and Feature *A* we have plotted a velocity-longitude diagram in Figure 2 which includes the theoretical model (dashed line) in the plane of the Galaxy for Feature *A* presented by Lindblad et al. (1973) and tentative velocities (open circles and squares) for the Orion "arm" or "other local feature" (OLF) which have been obtained from observations of various authors. Furthermore, we have plotted the velocities (crosses) of the dark clouds that we have observed at Onsala Space Observatory, Sweden, (Sandqvist et al., 1976) and NRAO, including the southern clouds reported in the present paper.

Although some clouds have velocities that are close to OLF's, a large majority of them show a distinct preference for the relation of Feature *A*. This preference is extremely pronounced in the region $30° > l > 335°$,

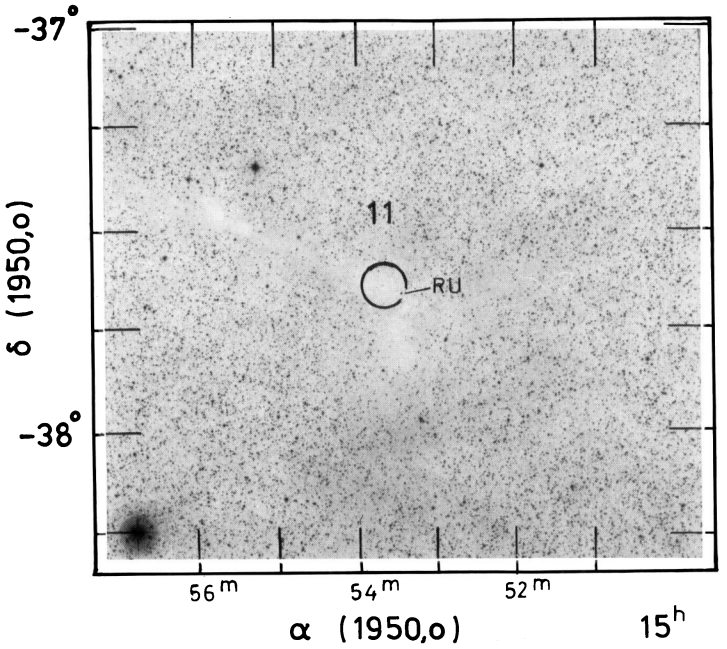


**Fig. 3.** Copy of a field from the Palomar Sky Atlas showing Cloud 11, RU Lup (RU) and the position of the 6.6 beam during the observations of the 6-cm $H_2CO$ line

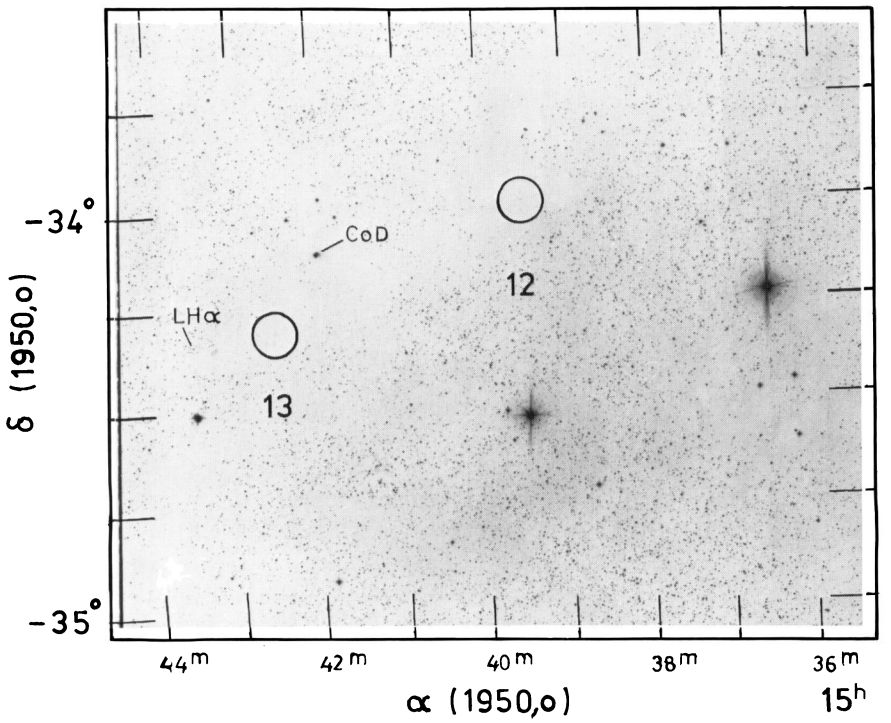


**Fig. 4.** Copy of a field from the Palomar Sky Atlas showing Clouds 12 and 13, CoD −33°10685 (CoD) and LHα 450-6 (LHα), and the positions of the 6.6 beam during the observations of the 6-cm $H_2CO$ line

a region which also contains the Heeschen cold cloud (CC), mapped in detail by Riegel and Crutcher (1972) using the H I line. Quirk and Crutcher (1973) have suggested that the CC is a region of high density in the very shock of the Orion "arm" but this is disputed by Rickard (1974) who places the CC near the shock of the Sagittarius arm. We believe that the CC and Feature *A* are physically related (Lindblad et al., 1973). The CC has major velocity components varying between +7 and +4 km s$^{-1}$ which for purely kinematical reasons seems to rule out its association with OLF which has a velocity of about +16 km s$^{-1}$ at $l=25°$ (one limit of the CC) and about −7 km s$^{-1}$ at $l=345°$ (the other limit of the CC). This does not explicitly rule out any possible association of the CC with a shock in the Orion "arm". However, the observational facts that (i) the CC's velocity-longitude relation follows so closely that of the majority of the dark clouds in the limited longitude range covered by the CC, and (ii) the clouds generally follow the relation of Feature *A*, would tend

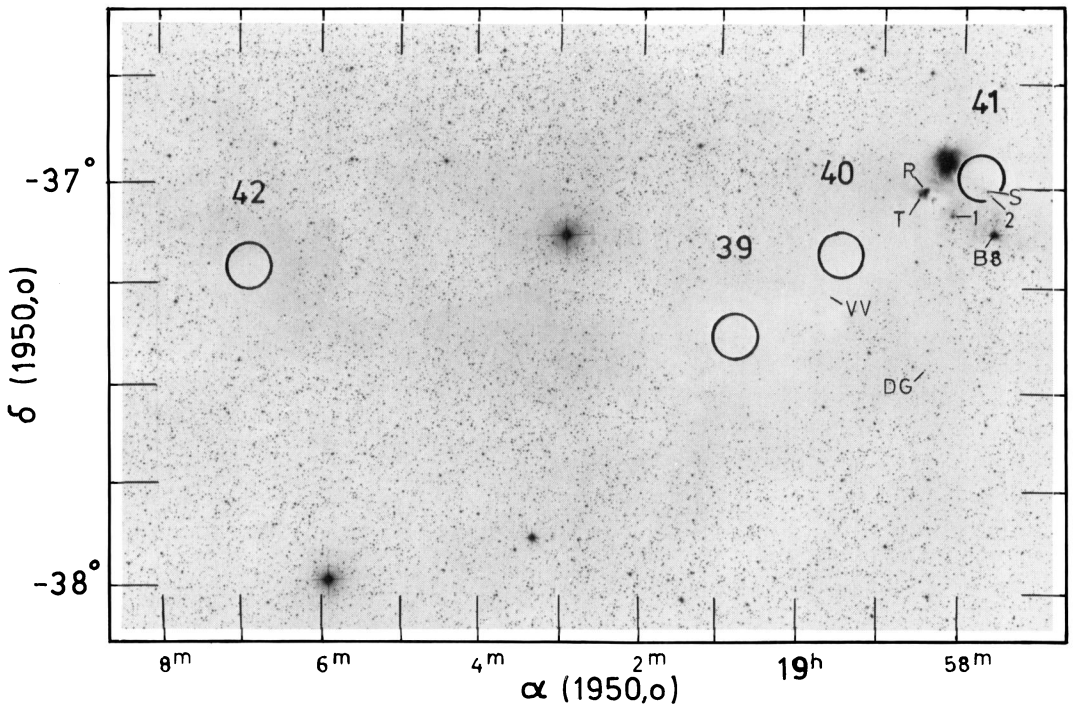


**Fig. 5.** Copy of a field from the Palomar Sky Atlas showing clouds 39, 40, 41 and 42, DG CrA (DG), R CrA (R), S CrA (S), T CrA (T) and VV CrA (VV) and the positions of the 6.′6 beam during the observations of the 6-cm $H_2CO$ line. B 8 is a group of double stars discussed in Section V(c), TY CrA is the illuminating star of the reflection nebula immediately to the northeast of position 41, and 1 and 2 are possible infrared sources discussed by Knacke et al. (1973)

to argue against the necessity for a local shock to explain only the part of Feature *A*'s velocity-longitude relationship which seems to be shared by the CC. The added observational fact that a number of the dark clouds, (which show kinematical behaviour similar to the CC's and Feature *A*'s), are at distances of the order of 150 pc, would tend to argue against the placing of this complex in the Sagittarius arm. This conclusion is further strengthened by Crutcher and Riegel (1974) finding a probable distance of about 150 pc to the CC and by Grape (1976) predicting a distance of the order of 100 pc to Feature *A* in the direction of the Galactic center.

Burton and Bania (1974) have attempted to interpret the behaviour of the local neutral hydrogen as a mere effect of the observer being immersed in a galactic flow pattern induced by a spiral gravitational potential. The predicted velocity-longitude relations of their model and Feature *A* differ significantly only in the fourth quadrant, precisely the quadrant where there is a dearth of observations. However, it can be seen in Figure 2 that at $l = 340°$ the model for Feature *A* predicts a radial velocity of about $+4\,\mathrm{km\,s^{-1}}$, a value close to that observed for the dark clouds and the CC, whereas the linear density wave model predicts a velocity of about $-7\,\mathrm{km\,s^{-1}}$ at this longitude, a velocity very close to that of OLF. Furthermore, Grape (1976) has discussed new H I data, obtained for the fourth quadrant, which strongly favours Feature *A* being a separate expanding subsystem. There is, however, some evidence that OLF may be explained by the Burton and Bania model.

In summary, we judge that the velocity-longitude relationships of the CC, most of the dark clouds, and Feature *A* imply a physical association of these three components of the local interstellar matter.

### *c) Dark Clouds and Emission-line Stars of the Orion Population*

Some of the observed dark clouds display an apparent association with emission-line stars of the Orion population type which are pre-main-sequence stars. We have chosen those Orion population stars in the catalogue of Herbig and Rao (1972) which are near the positions that we have observed in the 6-cm $H_2CO$ line and we have identified these stars and the formaldehyde positions on the Whiteoak Fields of the Palomar Sky Atlas seen in Figures 3–5.

As can be seen in Figure 3, Cloud 11 lies in the same direction as the T Tauri star, RU Lup, whose light variations have been interpreted by Gahm et al. (1975) as being due to dust concentrations of stellar dimensions crossing the line of sight to the star. These authors estimate that RU Lup lies at a distance of between 100 and 200 pc and it is very likely that the star is associated with Cloud 11, especially considering that the star's radial velocity of $+2.5\,\mathrm{km\,s^{-1}}$ is close to the $+4.7\,\mathrm{km\,s^{-1}}$

found for the cloud. If the dust concentrations are the cause of the light variations in RU Lup then their tangential velocity is about a hundred times higher than the general turbulent and thermal motion in Cloud 11 which is represented by the 0.25 km s$^{-1}$ velocity dispersion of the formaldehyde. This has lead Gahm et al. to consider the dust concentrations as most likely associated with the star, possibly gravitationally bound to it in the form of a protoplanetary system.

The CrA cloud complex with its high stellar birth activity is seen in Figure 5. Gaposchkin and Greenstein (1936) find 150 pc $\pm$ 50 as the most probable distance to this region and we obtain density estimates in the clouds of between $10^{-5}$ and $10^{-4}$ formaldehyde molecules cm$^{-3}$. It can be seen in Table 2 that the radial velocities for Clouds 42, 39 and 40 are about $+5.6$ km s$^{-1}$ whereas that for Cloud 41 is $+6.1$ km s$^{-1}$, a difference of 0.5 km s$^{-1}$ which is significant considering that the probable error is less than 0.1 km s$^{-1}$. This velocity gradient in the westermost part of the CrA cloud complex is illustrated (but not discussed) more clearly in Figure 1 of Loren et al. (1974). The velocity gradient, seen best in the optically thinner $^{13}C^{16}O$ line, begins approximately at the position of R CrA and the velocity increases westward gradually by about 1 km s$^{-1}$ reaching a maximum about a quarter of a degree west of R CrA after which it then decreases to the mean value for the whole region. The effect is somewhat similar to that of an arc expanding away from the observer. It is possible that radiation pressure from some of the newly formed and highly luminous stars like R CrA and TY CrA could be accelerating this part of the cloud complex, but the geometry of the situation is hard to conceive since the effect reaches a maximum west of these stars. However, there is a group of double stars, marked "B 8" in Figure 5, which may also play a part if they lie on the nearer side of the cloud. These two B 8-stars are designated BS 7169 and BS 7170 in the Bright Star Catalogue and the latter star is a spectroscopic binary. Distance estimates of about 200 pc to these stars place them near the upper limit of the distance to the CrA cloud, and some bright nebulosity on the cloudward side of the stars leads us to conclude that they are very close to the CrA cloud complex. That these B 8-stars may be interacting with the CrA cloud can be seen on the Whiteoak field $-36°18^{h}40^{m}$ where "B 8" is surrounded by an approximately elliptical "ring" of dark and faintly bright nebulosity, the ring measuring about $22' \times 30'$ with its long axis alligned north-sourth. It is just possible that "B 8" lies on the near side of the CrA cloud, exerts a radiation pressure on the cloud which causes it to accelerate by 1 km s$^{-1}$ in radial velocity with respect to the observer, and has a Strömgren sphere which is just barely visible on the Palomar Sky Atlas. This tentative picture is of course much in need of a detailed optical observational program being undertaken.

## VI. Conclusion

We have extended formaldehyde surveys of dark dust clouds further into the southern sky ($\delta > -46°$) and have found parameter values which are, not surprisingly, somewhat similar to those of more northern clouds. The small differences that we did find—e.g. smaller velocity dispersion and higher optical depth—we deem as due to our selecting only clouds of high visual opacity class and not as due to their peculiar positions of being in the direction of the Galactic center region. As can be seen from their small equivalent widths, the local clouds form a group distinctly different from the Galactic center group of molecular clouds which have very large equivalent widths. It is possible that the decrease in the number of clouds with low excitation temperature as the optical depth of the 6-cm $H_2CO$ line increases may be an effect predicted by the theory of the collisional cooling mechanism, i.e. that the excitation temperature should increase as the density in the cloud increases.

It is evident that at a distance of about 150 pc in the direction of the Galactic center region there is an increase in the density of the local interstellar matter—the dust clouds, the CC and Feature *A*. All three components show the tendency to lie above the galactic plane in this direction as do the O and B stars of Gould's Belt. Apparently isolated from this system at $b = -18°$, but with a similar radial velocity of $+5$ km s$^{-1}$, there is the CrA cloud complex with its stellar birth activity. For the solution of the many problems connected with this interesting region more detailed observing programs at both optical and radio wavelengths are needed.

*Acknowledgement.* We wish to thank Dr. P. O. Lindblad for stimulating discussions and for his interest in this project. We should also like to thank the National Radio Astronomy Observatory for granting observing time on the 42.7-m radio telescope. This work was supported by the Swedish Natural Science Research Council.

## References

Barnard, E. E.: 1927, Carnegie Institution of Washington Publications No. 247, Part 1
Burton, W. B., Bania, T. M.: 1974, *Astron. Astrophys.* **34**, 75
Crutcher, R. M., Riegel, K. W.: 1974, *Astrophys. J.* **188**, 481
Dieter, N. H.: 1973, *Astrophys. J.* **183**, 449
Evans, II, N. J., Zuckerman, B., Morris, G., Sato, T.: 1975, *Astrophys. J.* **196**, 433
Fomalont, E. B., Weliachew, L.: 1973, *Astrophys. J.* **181**, 781
Gahm, G. F., Nordh, H. L., Olofsson, S. G.: 1975, *Icarus* **24**, 372
Gaposchkin, S., Greenstein, J. L.: 1936, *Harvard Obs. Bull.* No. 904, 8
Grape, K.: 1976, to be published
Heiles, C.: 1973, *Astrophys. J.* **183**, 441
Herbig, G. H., Rao, N. K.: 1972, *Astrophys. J.* **174**, 401
Knacke, R. F., Strom, K. M., Strom, S. E., Young, E.: 1973, *Astrophys. J.* **179**, 847
Lindblad, P. O.: 1974, in L. N. Mavridis (Ed.), Stars and the Milky Way System, Springer, Berlin-Heidelberg-New York, p. 65

Lindblad, P. O., Grape, K., Sandqvist, Aa., Schober, J.: 1973, *Astron. & Astrophys.* **24**, 309
Loren, R. B., Peters, W. L., Vanden Bout, P. A.: 1974, *Astrophys. J. Letters* **194**, L 103
Lynds, B. T.: 1962, *Astrophys. J. Suppl.* **7**, 1
Minn, Y. K., Greenberg, J. M.: 1973, *Astron. & Astrophys.* **22**, 13
Quirk, W. J., Crutcher, R. M.: 1973, *Astrophys. J.* **181**, 359
Rickard, J. J.: 1974, *Astron. & Astrophys.* **31**, 47
Riegel, K. W., Crutcher, R. M.: 1972, *Astron. & Astrophys.* **18**, 55
Sandqvist, Aa.: 1974, *Astron. & Astrophys.* **33**, 413
Sandqvist, Aa., Lindblad, P. O.: 1976, to be published
Sandqvist, Aa., Lindblad, P. O., Lindroos, K. P.: 1976, in E. K. Kharadze (Ed.), Proceedings of the Third European Astronomical Meeting, Abastumani Astrophysical Observatory, p. 520
Scoville, N. Z., Solomon, P. M., Thaddeus, P.: 1972, *Astrophys. J.* **172**, 335
Tucker, K. D., Tomasevich, G. R., Thaddeus, P.: 1971, *Astrophys. J.* **169**, 429